

FIRST INFRARED BAND STRENGTHS FOR AMORPHOUS CO₂, AN OVERLOOKED COMPONENT OF INTERSTELLAR ICES

PERRY A. GERAKINES AND REGGIE L. HUDSON

Astrochemistry Laboratory, NASA Goddard Space Flight Center, Greenbelt, MD 20771 USA; Reggie.Hudson@NASA.gov

Received 2015 June 28; accepted 2015 July 6; published 2015 July 28

ABSTRACT

Solid carbon dioxide (CO₂) has long been recognized as a component of both interstellar and solar system ices, but a recent literature search has revealed significant qualitative and quantitative discrepancies in the laboratory spectra on which the abundances of extraterrestrial CO₂ are based. Here we report new infrared (IR) spectra of amorphous CO₂-ice along with band intensities (band strengths) of four mid-IR absorptions, the first such results in the literature. A possible thickness dependence for amorphous-CO₂ IR band shapes and positions also is investigated, and the three discordant reports of amorphous CO₂ spectra in the literature are addressed. Applications of our results are discussed with an emphasis on laboratory investigations and results from astronomical observations. A careful comparison with earlier work shows that the IR spectra calculated from several databases for CO₂ ices, all ices being made near 10 K, are not for amorphous CO₂, but rather for crystalline CO₂ or crystalline-amorphous mixtures.

Key words: astrochemistry – infrared: ISM – ISM: abundances – ISM: molecules – molecular data – planets and satellites: surfaces

1. INTRODUCTION

The analysis of astronomical spectra of interstellar and planetary ices continues to rely on laboratory spectra for the identification of molecules and ions. Such reference spectra must be accompanied by an unambiguous knowledge of ice composition, temperature, phase, history, and, to be applicable to the determination of molecular abundances, a quantitative measure of spectral intensity. As a specific case, recently we presented (Gerakines & Hudson 2015) new infrared (IR) results on solid methane (CH₄), an ice that has been studied spectroscopically for many years. We showed that the relatively few IR spectra published exhibit a lab-to-lab consistency, yet most if not all spectra reported are for a wholly or partially crystalline ice, and not the amorphous phase that might be expected near 10 K in the interstellar medium (ISM).

We now find that a similar study of frozen CO₂ is needed, motivated in part by the much greater interstellar abundance of CO₂ ices compared to CH₄ ices. In this paper we report new IR spectroscopic results on frozen CO₂, one of the more-common interstellar and planetary icy solids. Despite decades of attention paid to this molecular ice, and a voluminous associated literature, our new work appears to be the first to quantitatively characterize the IR spectra of carbon dioxide's amorphous phase.

Relatively few papers have addressed explicitly the IR spectra of amorphous CO₂, the first apparently being that of Falk (1987), who reported IR peaks at 2342.3 and 661.0 cm⁻¹. The band shapes of these features lacked the sub-structure known for crystalline ices, and warming of Falk's samples generated spectra that were said, but not shown, to be for the crystalline material. In contrast to his work stands that of Escribano et al. (2013) who reported amorphous-CO₂ spectra, but with IR peak positions at 2328 and 655 cm⁻¹, substantially different from those of Falk (1987). The thickness of the smallest ices of the former was on the order of a few nanometers compared to a few micrometers for the latter,

raising the possibility that some of the spectral variations were due to different ice thicknesses. Recently, Sivaraman et al. (2013) have reported experiments in which amorphous CO₂ was made at 30 K. Their peak positions for the strongest amorphous-CO₂ spectral features were listed (spectra not shown) at 2342.0, 661.6, and 655.2 cm⁻¹ which differ from those of both Falk (1987) and Escribano et al. (2013). Therefore, at present three sets of peak positions are in the literature for the same ice phase. This alone is a hindrance to applying such data to astronomical problems, but in addition none of these papers reported IR band intensities.

Adding to these uncertainties are questions surrounding the published CO₂-ice optical constants and associated spectra. Figure 1 compares IR transmission spectra for the ν_3 and ν_2 fundamentals of a CO₂ ice near 10 K as calculated for a thickness of 0.1 μm using the optical constants reported by four different research groups. Inspection of the traces in Figure 1 shows that there is both quantitative and qualitative disagreement in the results. Especially conspicuous is the splitting of the ν_2 band (~ 660 cm⁻¹, 15.2 μm), a CO₂ vibration long and often used to study conditions and chemical evolution in cold interstellar regions (e.g., d'Hendecourt & Jourdain de Mui-zon 1989; Pontoppidan et al. 2008; Cook et al. 2011). Over 60 years ago, Osberg & Hornig (1952) showed that such a splitting near 660 cm⁻¹ is expected from a factor-group analysis based on the crystal structure of CO₂. The implication is that each of the ices on which Figure 1 is based was partially or wholly crystalline, and so their associated optical constants provide no spectral-intensity information about amorphous CO₂.

Similar comments apply to IR spectra of CO₂ ices presented elsewhere in the astrochemical literature (e.g., Sandford & Allamandola 1990), making it doubtful that amorphous-CO₂ spectra were presented in them. In the recent papers of Rocha & Pilling (2014, 2015), CO₂-ice spectra, although reported to be for a sample grown near 13 K, were said to agree with those of Hudgins et al. (1993) and Ehrenfreund et al. (1997), but those authors' ices were crystalline. In still other papers (e.g.,

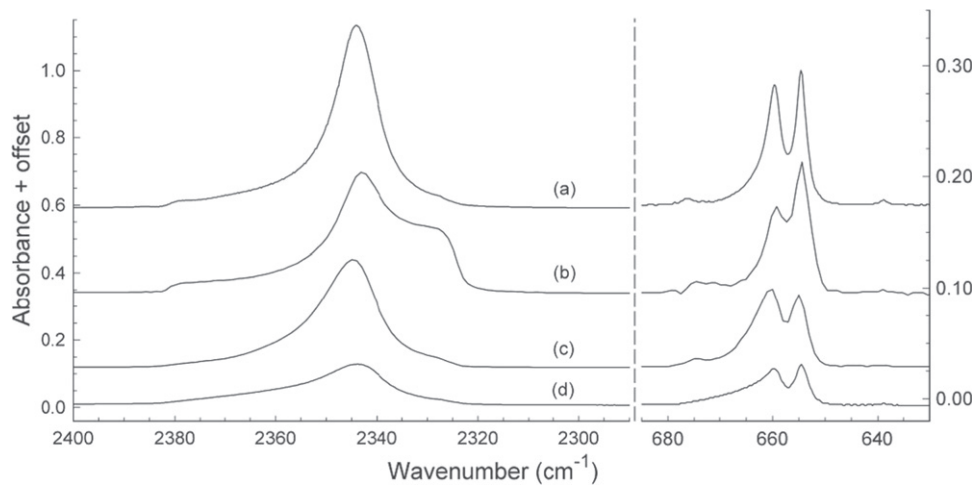


Figure 1. Infrared spectra of the ν_3 (left) and ν_2 (right) bands of CO_2 ices made near 10 K. The ice thickness was $0.10 \mu\text{m}$ in each case and the substrate chosen was KBr. Spectra were calculated (Swanepoel 1983) using the optical constants of (a) Ehrenfreund et al. (1997), (b) Hudgins et al. (1993), (c) Baratta & Palumbo (1998), and (d) Rocha & Pilling (2014). Spectra are offset for clarity.

Bennett et al. 2014), the IR reflection technique employed to acquire data, along with the small scale of the spectra presented, make an independent evaluation of phase and the extraction of band intensities for amorphous CO_2 difficult.

Our conclusion is that despite the relatively high interstellar abundance of solid CO_2 , and an extensive associated literature, astrochemists still lack a mid-IR spectrum of amorphous CO_2 accompanied by a set of band strengths. Without such information for amorphous CO_2 , applications to solid-state astrochemistry will be highly problematic. Therefore in this letter we describe our first results on amorphous CO_2 and its IR spectrum, all based on new laboratory measurements. We present new spectra of CO_2 ices whose phase can be unambiguously assigned, accompanied by newly determined band strengths. Finally, we consider some important CO_2 -ice publications in light of our new results and comment on how our results will be useful.

2. EXPERIMENTAL METHOD

The procedures and equipment used were similar to those of our recent CH_4 investigation (Gerakines & Hudson 2015; Hudson et al. 2015). The main difference between the work reported here and that from earlier CO_2 studies in other laboratories appears to be the slower rate at which our ices were grown by gas-phase condensation. The rates we used gave an increase in each sample's thickness of about $0.1 \mu\text{m hr}^{-1}$. Doubling this rate gave crystalline CO_2 ices even at a deposition temperature of 10 K. Ice thicknesses were determined by laser interferometry using a reference index of refraction of $n(670 \text{ nm}) = 1.30$. To calculate IR band strengths, denoted A' , a density $\rho = 1.28 \text{ g cm}^{-3}$ was used, giving $1.751 \times 10^{22} \text{ molecules cm}^{-3}$ as the CO_2 number density. Both $n(670 \text{ nm})$ and ρ were measured three times with CO_2 at 14 K in our laboratory with equipment and methods similar to those of Satorre et al. (2008), and with details to be supplied in a future paper. See also our similar measurements of n in Moore et al. (2010).

IR spectra were recorded as 100 scan accumulations with a resolution of 0.2 cm^{-1} on a KBr substrate in a high-vacuum chamber (10^{-7} – 10^{-8} torr). A resolution of 1 cm^{-1} gave essentially the same band intensities for our amorphous

samples, but with lower noise, and so sometimes was employed for quick checks on the quality of a sample. The CO_2 used was obtained from Matheson Tri-Gas (Research Purity, 99.999%) Cambridge Isotope Laboratories (isotopic purity 99%). The chief contaminant seen was residual H_2O from the CO_2 reagents and possibly from our vacuum system. Trace amounts of H_2O gave weak IR peaks (<0.01 absorbance units in all cases) in the 3700 – 3500 and 1600 cm^{-1} regions, far from the IR features of interest.

Uncertainties in our reported results are similar to those in our work on C_2H_2 , C_2H_4 , C_2H_6 , and CH_4 (Hudson et al. 2014a, 2014b; Gerakines & Hudson 2015; Hudson et al. 2015) and are given in the table presented later in this paper.

3. RESULTS

Experiments began with the condensation at 10 K of room-temperature CO_2 gas to produce solid CO_2 . Spectrum (a) of Figure 2 shows expansions of such an ice's ν_3 (left) and ν_2 (right) regions. Spectrum (b) was obtained by warming this same sample to 70 K and then recooling to 10 K. Close agreement was found between (b) and the spectra of crystalline CO_2 reported by Yamada & Person (1964), and when we deposited CO_2 at 60 K there was essentially perfect agreement for the band shapes and positions. Assigning spectrum (b) to crystalline CO_2 suggests that its precursor, spectrum (a), is that of amorphous CO_2 . Supporting this assignment is the method used (slow condensation) to make the ice corresponding to (a), this spectrum's irreversible conversion to that of crystalline CO_2 on warming, and spectrum (a)'s lack of sharp substructure for the ν_2 and ν_3 features.

The left-hand side of Figure 3 shows the result of separate, independent CO_2 depositions at 10 K for four sample thicknesses. As expected, in each spectral region an increasingly intense IR band was seen for increasingly thicker ices. Expansions around 1384 and 1277 cm^{-1} (not shown) revealed the weak ν_1 and $2\nu_2$ Fermi resonance features. Since ν_1 (symmetric stretching vibration) is IR-forbidden in the crystalline phase, its presence supports our assignment of these spectra to amorphous CO_2 . See Hudson et al. (2015) for the activation of forbidden transitions in other amorphous ices.

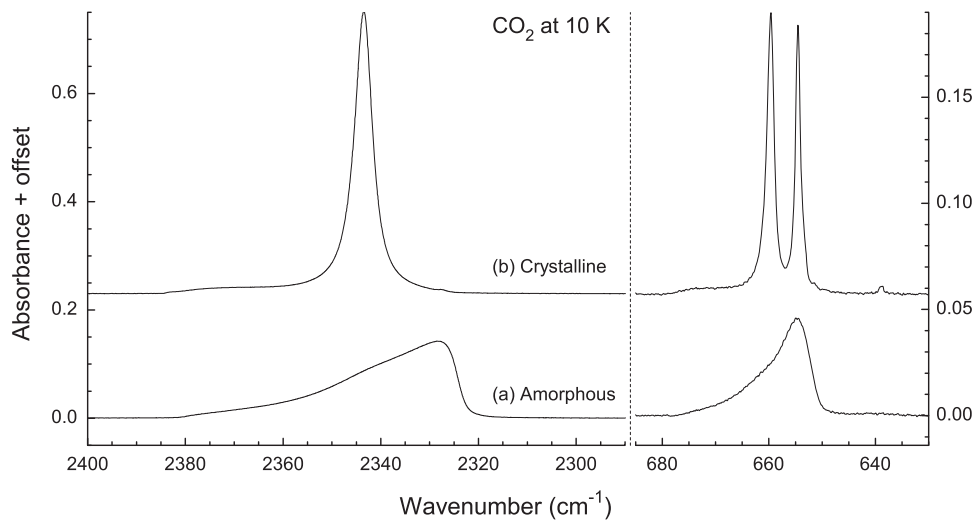


Figure 2. Infrared spectra of the ν_3 (left) and ν_2 (right) bands of solid CO_2 . The CO_2 ice sample was grown at 10 K to give (a) an amorphous solid that (b) crystallized on warming to 70 K and then was recooled to 10 K to give the spectrum shown. The thickness of the initial sample was about $0.03 \mu\text{m}$. Spectra are offset for clarity.

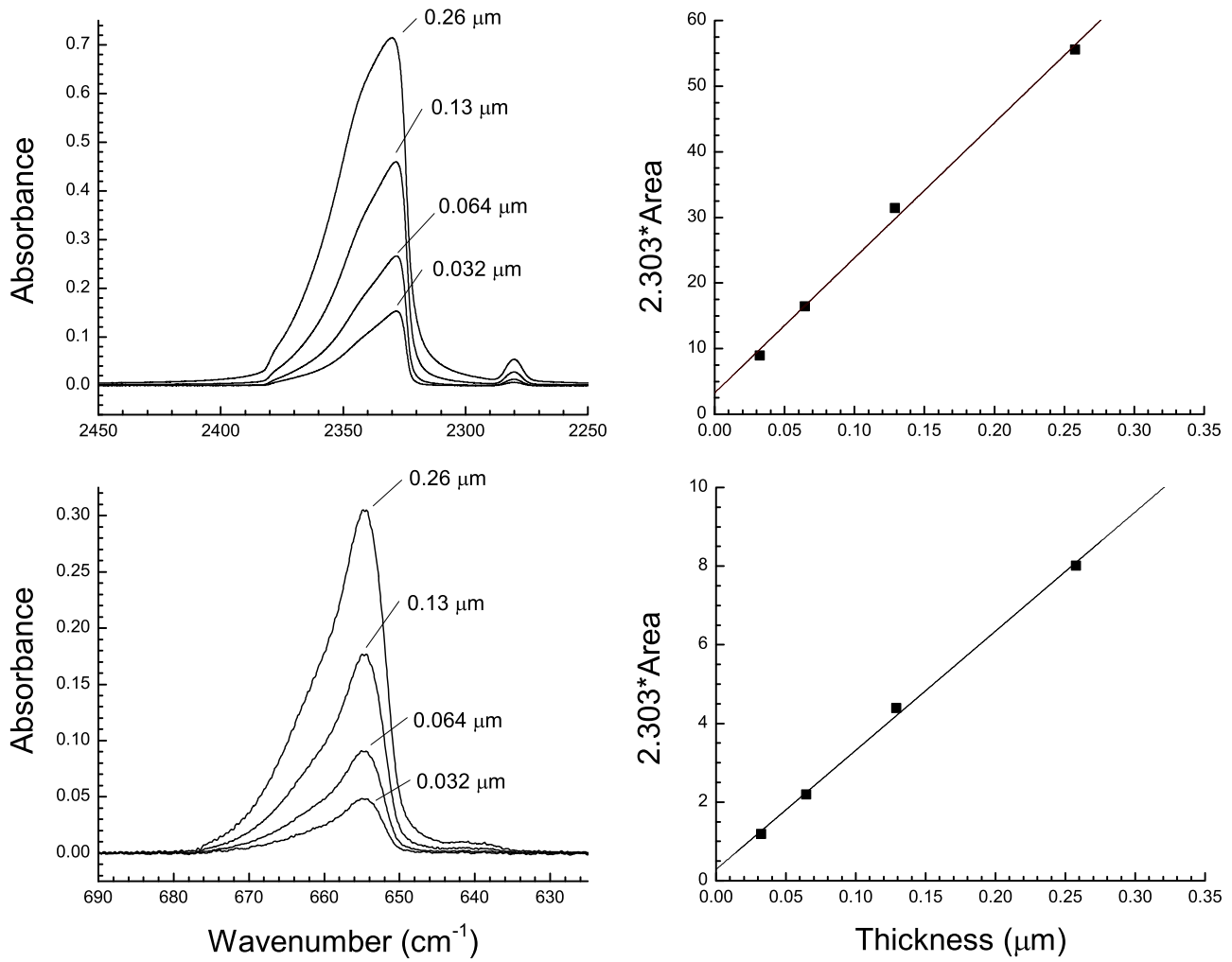


Figure 3. Left: infrared spectra of amorphous CO_2 ices at 10 K at the thicknesses listed. Right: Beer's law plots of integrated optical depth as a function of ice thickness for the spectra shown at the left. Note that integrated optical depth equals $2.303 \times$ integrated absorbance (i.e., band area) and that the slope of each graph is $\rho_N A'$ for the corresponding IR band. The vertical axis of each of the two right plots has units of cm^{-1} .

Table 1
IR Features of Amorphous CO₂ at 10 K^a

Property	$\nu_1 + \nu_3$	$2\nu_2 + \nu_3$	ν_3	ν_2
$\bar{\nu}/\text{cm}^{-1}$	3704	3597	2329	654.7
$\lambda/\mu\text{m}$	2.700	2.780	4.294	15.27
FWHM/ cm^{-1}	9.8	7.1	27.1	9.2
α'/cm^{-1}	3890 ± 40	1557 ± 18	$71,710 \pm 3,016$	$30,380 \pm 131$
$\rho_N A'/\text{cm}^{-2}$	$70,980 \pm 1490$	$21,860 \pm 372$	$2,058,000 \pm 84,130$	$302,900 \pm 9363$
$A'/\text{cm molecule}^{-1}$	$4.05 \pm 0.10 \times 10^{-18}$	$1.25 \pm 0.02 \times 10^{-18}$	$1.18 \pm 0.05 \times 10^{-16}$	$1.73 \pm 0.53 \times 10^{-17}$
Integration range/ cm^{-1}	3762–3645	3643–3577	2420–2290	680–630

Note.

^a FWHM; α' and A' denote apparent absorption coefficient and apparent band strength taken directly from a set of IR spectra using Beer's law type plots; values of n (670 nm) = 1.30 and $\rho = 1.28 \text{ g cm}^{-3}$, or $\rho_N = 1.751 \times 10^{22} \text{ molecules cm}^{-3}$, for CO₂ were used throughout.

A few measurements were carried out with ¹³CO₂, and the results mirrored those of our ¹²CO₂ experiments. The peak positions for the stronger fundamentals for amorphous ¹³CO₂ at 10 K were 2263.4 and 636.3 cm⁻¹ for ν_3 and ν_2 , respectively, giving ¹³C shifts of 66.4 and 18.4 cm⁻¹.

4. DISCUSSION

The CO₂-ice IR spectra of Figures 2 and 3 possess many characteristics of interest, but in this paper we focus our attention on spectral profiles and intensities.

4.1. IR Spectra of Amorphous CO₂

Figure 2 shows distinct differences in the band shapes, intensities, and positions for the amorphous and crystalline phases of solid CO₂, and these results can be used to judge the presence or absence of crystalline material. One such difference is the splitting near 660 cm⁻¹, which can be taken as a reliable indicator of crystallinity because no such splitting is present in purely amorphous CO₂ samples. A second difference between the IR spectra of amorphous and crystalline CO₂ ices is the asymmetry of the ν_2 and ν_3 features. Similar band shapes have been reported in the IR spectra of other molecular solids by us and others (Ovchinnikov & Wight 1993; Hudson et al. 2014a).

Concerning the aforementioned disagreements in the amorphous-CO₂ literature, our work best matches the results of Escribano et al. (2013), and it also extends them. Their amorphous CO₂ ices were on the order of nanometers in thickness, whereas our results show that micrometer sizes can be reached with little degradation of the spectral band profiles. Our results disagree, however, with the band positions of both Sivaraman et al. (2013) and Falk (1987). For the former, we suspect that their ice actually was crystalline, or partly so, based on their 30 K deposition temperature and the fact that two peaks were listed near 660 cm⁻¹, and not the single peak of our Figures 2 and 3. Since no deposition rate was stated and no spectra were shown for the crucial ν_2 region, little more can be deduced. As already stated, the key laboratory parameter for making amorphous CO₂ appears to be a slow rate of growth for the ice, a condition that is expected for many astronomical environments. Concerning the spectra of Falk (1987), the profiles of his CO₂-ice features resemble ours, but his peak positions for the amorphous solid are off for both ¹²CO₂ and ¹³CO₂ ices. Since his isotopic shifts and crystalline-CO₂ peak positions are about the same as ours, we suspect either a

calibration error or a mislabeling of his wavenumber scale for the amorphous-CO₂ features.

Although this paper is focused on amorphous CO₂, a few comments on the spectrum of crystalline CO₂ in Figure 2 are appropriate, starting with the pronounced splitting near 660 cm⁻¹ for the crystalline ice. This sub-structure arises from the symmetry change on going from the $D_{\infty h}$ point group of gas-phase CO₂ molecules to the Pa3 space group of crystalline CO₂, and with selection rules that are further altered in the amorphous phase. Explanations of the IR spectra observed in the crystalline case follow from a factor-group analysis and lead to an expectation of two separate features for the CO₂ molecule's ν_2 band, and Figure 2 shows that that prediction is confirmed. See Dahlke (1936) for early hints of such splitting, and full confirmation in Osberg & Hornig (1952) and many later papers. Isokoski et al. (2013) recently studied this same ν_2 feature of crystalline CO₂ and our results agree closely with theirs, even giving the same ratios that they graphed for the maximum and minimum near 660 cm⁻¹ as a function of temperature.

4.2. IR Band Strengths of Amorphous CO₂

The method of Hollenberg & Dows (1961) was used to derive IR band strengths. Rearranging their equation to give

$$(2.303) \int_{\text{band}} (\text{Absorbance}) d\bar{\nu} = (\rho_N A') h \quad (1)$$

shows that for the spectra on the left-hand side of Figure 3, a graph of $2.303 \times$ (integrated absorbance) as a function of thickness (h) will be a straight line with slope $\rho_N A'$, where ρ_N is the number density (molecules cm⁻³) of CO₂ molecules in the sample and A' is the apparent band strength. The right-hand side of the same figure shows the resulting plots for two amorphous-CO₂ features. Slopes are given in Table 1 along with the resulting values of A' . Similar graphs of $2.303 \times$ (peak height) as a function of thickness gave apparent absorption coefficients (α'), also listed in Table 1. See Hudson et al. (2014a, 2014b and references therein) for additional details, including the differences between apparent and absolute intensities.

Figure 3 also shows that the band positions and profiles of amorphous-CO₂ IR spectra do not undergo significant shifts with ice thickness, unlike the case of, for example, crystalline C₂H₂ (Hudson et al. 2014a). This means that the band strengths (A') listed for each amorphous-CO₂ IR band in Table 1 should

be applicable without modification to a wide variety of interstellar and planetary-science situations.

For applications to interstellar chemistry, perhaps the most important A' in Table 1 is $A'(\nu_3) = 1.18 \times 10^{-16}$ cm molecule $^{-1}$. Most values now in the astrochemical literature are smaller and can be traced to older work on crystalline CO $_2$ at higher temperatures. For example, $A'(\nu_3)$ values near 7.7×10^{-17} cm molecule $^{-1}$ were used by Lv et al. (2012), who cited Jamieson et al. (2006) who cited Gerakines et al. (1995), who relied on the original measurement of this value by Yamada & Person (1964) for crystalline CO $_2$ near 80 K. The $A'(\nu_3)$ value we are reporting for amorphous CO $_2$ near 10 K is about 53% larger than that of Yamada & Person (1964) for crystalline CO $_2$ near 80 K.

4.3. Astrochemical Applications and Implications

The immediate result of our work is that the mid-IR spectrum of amorphous CO $_2$ is now available, accompanied by band strengths and a knowledge that the accompanying band profiles and positions do not change substantially over the nanometer-to-micrometer range. There are several areas where these results can be important. First, an A' value for crystalline CO $_2$ ice has been used in many laboratory studies to calculate abundances of starting materials and of reaction products (e.g., Mennella et al. 2006; Peeters et al. 2010). Our new A' values (Table 1) will necessitate reevaluations of some of those earlier results, particularly those involving amorphous ices. Similarly, previous laboratory work in which abundance ratios, such as CO/CO $_2$, were calculated may need reassessing (e.g., Pilling et al. 2011). Also, kinetic studies that rely on CO $_2$ abundances, such as for a mass balance, almost certainly need revisiting (e.g., de Barros et al. 2014). Our IR spectra can be useful when comparisons might benefit from data on amorphous CO $_2$, as opposed to crystalline CO $_2$ (Iopollo et al. 2009, 2013; Lv et al. 2014). Edridge et al. (2013) allude to the unexpected observation of an IR feature near 2381 cm $^{-1}$ in work on amorphous CO $_2$ by others, this particular band being more expected for a crystalline ice. However, Figure 7 of that earlier study (Baratta & Palumbo 1998) shows a double-peaked feature near 660 cm $^{-1}$, and so according to our Figure 2 the sample used was partially or wholly crystalline CO $_2$, explaining the 2381 cm $^{-1}$ feature (Parker & Eggers 1966).

Beyond these laboratory applications, IR band profiles of solid CO $_2$ have been used extensively in attempts to fit IR spectra of interstellar ices. Such fits, from which CO $_2$ -ice abundances are derived, may need reassessing in light of the significant differences we have found in the band profiles and intensities of amorphous and crystalline CO $_2$ (Figure 2). As an example, Figure 4 contains a fit to the 15 μ m *Spitzer Space Telescope* spectrum observed toward the background field star Q21-1, a line of sight that probes the dense ISM in the cold dark cloud IC 5146 (data from Whittet et al. 2009). Two laboratory components are included in roughly a 10:1 ratio, H $_2$ O + CO $_2$ + CO = 100:20:3 at 20 K (Ehrenfreund et al. 1996) and amorphous CO $_2$ at 10 K (this study), respectively. The resulting best-fitting combination shown in Figure 4 suggests that up to \sim 9% of the solid CO $_2$ in this line of sight may be amorphous. Previous studies using laboratory fits to interstellar quiescent-cloud CO $_2$ spectra conclude that the non-polar component is either a CO- or CO $_2$ -dominated ice mixture.

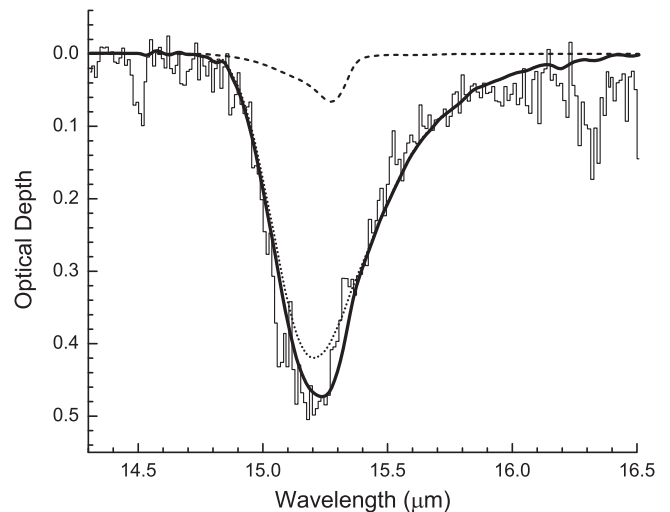


Figure 4. The optical depth spectrum of a dark interstellar cloud toward the background field star Q21-1. Thin solid histogram: *Spitzer* spectrum from Whittet et al. (2009); dotted line: laboratory spectrum of H $_2$ O + CO $_2$ + CO (100:20:3) from Ehrenfreund et al. (1996); dashed line: laboratory spectrum of amorphous CO $_2$ at 10 K (this work); thick solid line: sum of the laboratory spectra.

Concerning IR band strengths, those now in widest use for amorphous CO $_2$ -containing mixtures near 10 K (Gerakines et al. 1995) derive from measurements on pure crystalline CO $_2$ near 80 K (Yamada & Person 1964), scaled with ice composition. Our band strengths measured near 10 K for amorphous CO $_2$ could be more appropriate to use in such cases.

5. CONCLUSION

An accurate, quantitative spectroscopic characterization of amorphous CO $_2$ has been presented. Our new IR transmission spectra, such as in Figures 2 and 3, will help to distinguish amorphous and crystalline CO $_2$ ice phases through band positions, widths, and shapes. However, just as important are the band intensities in our Table 1, which can be used to derive CO $_2$ abundances in ices and, in turn, deduce evolutionary and environmental information, such as thermal histories. We also suggest that a primary reason for the confusion and disagreement among the spectra of Figure 1, and other such data (e.g., Poteet et al. 2013), is that the various ice samples used were not of a single CO $_2$ phase, but for amorphous-crystalline mixtures. A fresh opportunity now presents itself to accurately reassess the role of frozen CO $_2$ in planetary and interstellar ices and the information it can convey about its surroundings. Spectra are posted on our group's web site.¹

NASA funding through the Astrophysics Research and Analysis, Cassini Data Analysis, and Outer Planets Research programs is acknowledged. Both authors received partial support from the NASA Astrobiology Institute through the Goddard Center for Astrobiology. Mark Loeffler is particularly acknowledged for constructing the ultra-high vacuum system with which he and Marla Moore measured n and ρ . Robert Ferrante and Tatiana Tway are thanked for assistance with IR measurements.

¹ <http://science.gsfc.nasa.gov/691/cosmicice/constants.html>

REFERENCES

- Baratta, G. A., & Palumbo, M. E. 1998, *JOSA*, 15, 3076
- Bennett, C. J., Ennis, C. P., & Kaiser, R. I. 2014, *ApJ*, 794, 57
- Cook, A. M., Whittet, D. C. B., Shenoy, S. S., et al. 2011, *ApJ*, 730, 124
- Dahlke, W. 1936, *ZPhy*, 102, 360
- de Barros, A. L. F., da Silveira, E. F., Pilling, S., et al. 2014, *MNRAS*, 438, 2026
- d'Hendecourt, L. B., & Jourdain de Muizon, M. 1989, *A&A*, 223, L5
- Edridge, J. L., Freimann, K., Burke, D. J., & Brown, W. A. 2013, *RSPTA*, 371, 20110578
- Ehrenfreund, P., Boogert, A. C. A., Gerakines, P. A., et al. 1996, *A&A*, 315, L341
- Ehrenfreund, P., Boogert, A. C. A., Gerakines, P. A., Tielens, A. G. G. M., & van Dishoeck, E. F. 1997, *A&A*, 328, 649
- Escribano, R. M., Muñoz Caro, G. M., Cruz-Díaz, G. A., Rodríguez-Lazcano, Y., & Matéa, B. 2013, *PNAS*, 110, 12899
- Falk, M. 1987, *JChPh*, 88, 560
- Gerakines, P. A., & Hudson, R. L. 2015, *ApJL*, 805, L20
- Gerakines, P. A., Schutte, W. A., Greenberg, J. M., & van Dishoeck, E. F. 1995, *A&A*, 296, 810
- Hollenberg, J., & Dows, D. A. 1961, *JChPh*, 34, 1961
- Hudgins, D. M., Sandford, S. A., Allamandola, L. J., & Tielens, A. G. G. M. 1993, *ApJS*, 86, 713
- Hudson, R. L., Ferrante, R. F., & Moore, M. H. 2014a, *Icar*, 228, 276
- Hudson, R. L., Gerakines, P. A., & Loeffler, M. J. 2015, *PCCP*, 17, 12545
- Hudson, R. L., Gerakines, P. A., & Moore, M. H. 2014b, *Icar*, 243, 148
- Iopollo, S., Palumbo, M. E., Baratta, G. A., & Mennella, V. 2009, *A&A*, 493, 1017
- Iopollo, S., Sangiorgio, I., Baratta, G. A., & Palumbo, M. E. 2013, *A&A*, 554, A34
- Isokoski, K., Poteet, C. A., & Linnartz, H. 2013, *A&A*, 555, A85
- Jamieson, C. S., Mebel, A. M., & Kaiser, R. I. 2006, *ApJS*, 163, 184
- Lv, X. Y., Boduch, P., Ding, J. J., et al. 2014, *PCCP*, 16, 3433
- Lv, X. Y., de Barros, A. L. F., Boduch, P., et al. 2012, *A&A*, 546, A81
- Mennella, V., Baratta, G. A., Palumbo, M. E., & Bergin, E. A. 2006, *ApJ*, 643, 92
- Moore, M. H., Ferrante, R. F., Moore, W. J., & Hudson, R. L. 2010, *ApJS*, 191, 96
- Osberg, W. E., & Hornig, D. F. 1952, *JChPh*, 20, 1345
- Ovchinnikov, M. A., & Wight, C. A. 1993, *JChPh*, 99, 3374
- Parker, M. A., & Eggers, D. F., Jr. 1966, *JChPh*, 45, 4354
- Peeters, Z., Hudson, R. L., Moore, M. H., & Lewis, A. 2010, *Icar*, 210, 480
- Pilling, S., Duarte, E. S., Domaracka, A., et al. 2011, *PCCP*, 13, 15755
- Pontoppidan, K. M., Boogert, A. C. A., Fraser, H. J., et al. 2008, *ApJ*, 678, 1005
- Poteet, C. A., Pontoppidan, K. M., Megeath, T., et al. 2013, *ApJ*, 766, 117
- Rocha, W. R. M., & Pilling, S. 2014, *AcSpe*, 123, 436
- Rocha, W. R. M., & Pilling, S. 2015, *ApJ*, 803, 18
- Sandford, S. A., & Allamandola, L. J. 1990, *ApJ*, 355, 357
- Satorre, M. Á., Domingo, M., Millán, C., et al. 2008, *PSS*, 56, 1748
- Sivaraman, B., Raja Sekhar, B. N., Fulvio, D., et al. 2013, *JChPh*, 139, 074706
- Swanepoel, R. 1983, *JPhE*, 16, 1214
- Whittet, D. C. B., Cook, A. M., Chiar, J. E., et al. 2009, *ApJ*, 695, 95
- Yamada, H., & Person, W. B. 1964, *JChPh*, 41, 2478